

# FINAL DESIGN REVIEW FOR THE SILICON DETECTORS OF THE ATLAS SCT

## ATLAS SCT/Detector FDR/99-5

### Baseline module designs and thermal simulations

#### 1. Barrel and Forward module parameters

For the SCT barrel, the required tracking precision is obtained by modules with an intrinsic point resolution of  $23\text{ }\mu\text{m}$  in the  $r$ - $\phi$  coordinate per single side measurement. The precision is obtained for the binary readout scheme (on-off readout) using detectors with  $80\text{ }\mu\text{m}$  readout pitch. A back-to-back detector pair with a stereo rotation angle of  $40\text{ mrad}$  gives a precision of  $17\text{ }\mu\text{m}$  in the  $r$ - $\phi$  coordinate and  $500\text{ }\mu\text{m}$  in the  $z$  coordinate from the correlations obtained through fitting.

The severity and consequences of the high accumulated radiation levels for silicon detector operation, causing increased leakage current and type inversion, give rise to the need to operate detectors at  $-7^\circ\text{C}$ . The maximum expected fluence after 10 years of operation in the SCT is  $2 \times 10^{14}\text{ 1 MeV-neutron-equivalent/cm}^2$  (at the upper limit of uncertainty of 50% in the total cross section). The corresponding depletion voltage will be in the range 300-400 volts depending upon warm-up scenarios. This will result in a total leakage current of  $\sim 0.7\text{ mA}$  for a barrel detector operated at  $-7^\circ\text{C}$  at a bias voltage of 350 V. The leakage current is dependent on temperature, roughly twice per  $7^\circ\text{C}$ . The detector heat generation requires the knowledge of the temperature of the detectors in the module.

Thermal considerations, and especially concerns of thermal run-away, lead to a module design where the effective in-plane thermal conductivity must be increased beyond that of silicon. In practice this will be achieved by the use of thermal heat spreading materials which are laminated as part of the detector sandwich.

The power consumption of the frontend LSI chips are expected to be 5.5 W nominal and 7.2 W maximum. The thermal design of the module must allow for this.

The mechanical tolerance for positioning wafers within the back-to-back pair must be  $\sim 5\text{ }\mu\text{m}$  in lateral strip position,  $\sim 50\text{ }\mu\text{m}$  in module thickness, and  $\sim 25\text{ }\mu\text{m}$  in  $z$ . The forward region measures the longitudinal momentum and the track dip angle. The requirements are very similar to the barrel after allowing for interchange of  $r$  and  $z$ .

The SCT will undergo temperature cycling over the range  $-20^\circ\text{C}$  to  $+25^\circ\text{C}$  in a controlled sequence, and it must be safe, in the event of cooling or local power fluctuations, at temperatures up to  $50^\circ\text{C}$ . This requires the module design to have minimal CTE, and to be capable of elastic deformation. The precision of the tracking measurement depends on the modules having a stable profile after changes of the operating conditions. To prevent fracture, permanent deformations should be  $< 5\text{ }\mu\text{m}$ , and elastic deformations occurring across the full temperature range should be  $< 50\text{ }\mu\text{m}$ .

The modules parameters are summarized in Table 1-1 and Table 1-2.

**Table 1-1** Barrel module parameters

<b>Silicon outer dimension (cut-edge)</b>	<b>63.56 mm x 128.05 mm</b>
Construction	Four 63.56 mm x 63.96 mm <i>p-on-n</i> single sided detectors to form back-to-back glued detectors
Mechanical tolerance	back-to-back: <5 $\mu\text{m}$ ( $\phi$ ), <50 $\mu\text{m}$ (r), <25 $\mu\text{m}$ (z) Fixation point: <50 $\mu\text{m}$ ( $\phi$ ), <100 $\mu\text{m}$ (z)
Strip length	126.09 mm (2.090 mm dead in the middle)
Strip directions	$\pm 20$ mrad (0, $\pm 40$ mrad on support structure)
Number of readout strips	768 per side, 1536 total
Strip pitch	80 $\mu\text{m}$
Hybrid	two single-sided hybrids bridged over the detector
Hybrid power consumption	5.5 W nominal, 7.2 W maximum
Maximum detector bias voltage	350 V (on the detector), up to 410 V in the module
Operating temp. of detector	-7°C (average)
Uniformity of silicon temp.	<5°C
Detector power consumption	1 W /total at -7 °C, Heat flux (300 $\mu\text{m}$ ): 120 $\mu\text{W}/\text{mm}^2$ at 0°C
Thermal runaway	Heat flux : >240 $\mu\text{W}/\text{mm}^2$ at 0 °C
Permanent deformation	<5 $\mu\text{m}$ (after 10 thermal cycles between -20 and +70°C)
Power on-off deformation	<10 $\mu\text{m}$ (Detector & Hybrid)
Dynamical deformation	<50 $\mu\text{m}$ (between -20 and +30°C)

After considering the combined electrical, thermal and mechanical requirements, the optimised modules will use centre-tap hybrid readout in the barrel region and end-tap for the forward region.

## 2. Description of module designs

### 2.1 The barrel module

In the barrel region, one module is made of four 63.96 mm x 63.56 mm (cut-edge size) single-sided silicon microstrip detectors. Geometrical dimensions are shown in Figure 2-2 for two detectors butt joined to form a 128 mm long mechanical unit. Strips of two of the detectors are electrically connected to form 126 mm long strips. In order to form a double-sided readout module, two 128 mm long mechanical units are back-to-back aligned and glued with a stereo angle of 40 mrad. One side of the module measures the  $r$ - $\phi$  coordinates ("axial strips") while the other side measures the 40 mrad rotated coordinate (the "stereo strips"). The pitch of the strips

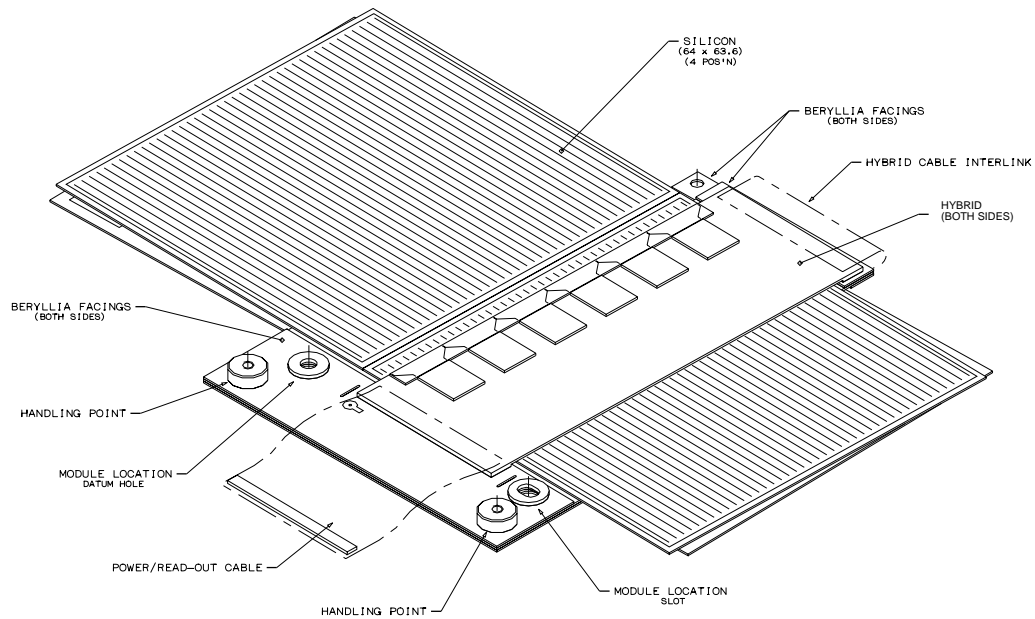
**Table 1-2** Forward module parameters

<b>Silicon outer dimension (cut-edge)</b>	<b>Outer: 56.475- 71.814 mm x 123.195 mm Middle: 55.734- 74.847 mm x 119.660 mm Half-middle: 66.152 - 74.847 mm x 54.435 mm Half-inner: 43.662 - 55.488 mm x 74.040 mm</b>
Construction	Four wedge-shaped <i>p-on-n</i> single sided detectors to form back-to-back glued detectors in the outer and the middle, two detectors back-to-back in the half-middle and half-inner modules
Mechanical tolerance	back-to-back: <5 $\mu\text{m}$ ( $\phi$ ), <50 $\mu\text{m}$ (z), <25 $\mu\text{m}$ (r) Fixation point: <50 $\mu\text{m}$ ( $\phi$ ), <100 $\mu\text{m}$ (r)
Strip length	Outer: 121.235 mm (2.100 mm dead near the middle) Middle: 117.700 mm (2.100 mm dead near the middle) Half-middle: 52.475 mm, Half-inner: 72.100 mm
Strip directions	$\pm 20$ mrad, (0, $\pm 40$ mrad Fan at support structure)
Number of readout strips	768/side, 1536/total
Strip pitch	Outer: 70.9 - 90.4 $\mu\text{m}$ , Middle: 69.9 - 94.3 $\mu\text{m}$ , Half-middle: 83.5 - 94.3 $\mu\text{m}$ , Half-inner: 54.2 - 69.2 $\mu\text{m}$
Hybrid	one double-sided hybrid, set at one end of module
Hybrid power consumption	5.5 W nominal, 7.2 W maximum
Maximum detector bias voltage	350 V (at the detector), up to 410 V in the module
Operating temp. of detector	-7°C (average)
Uniformity of silicon temp.	<5°C
Detector power consumption	1 W/total at -7 °C, Heat flux : 120 $\mu\text{W}/\text{mm}^2$ at 0 °C
Thermal runaway	Heat flux : >240 $\mu\text{W}/\text{mm}^2$ at 0 °C
Permanent deformation	<5 $\mu\text{m}$ (after 10 thermal cycles between -20 and +70°C)
Power on-off deformation	<10 $\mu\text{m}$ (Detector & Hybrid)
Dynamical deformation	<50 $\mu\text{m}$ (between -20 and +30°C)

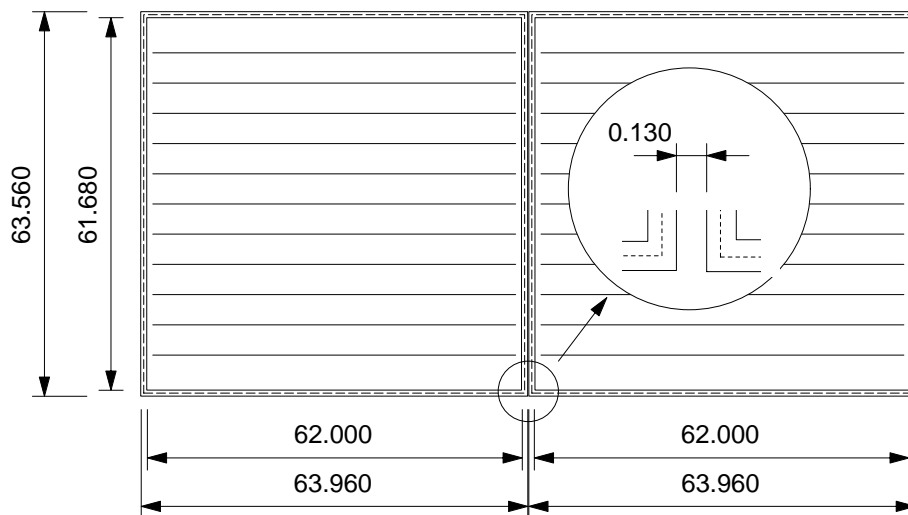
is 80  $\mu\text{m}$  and there are 770 strips per plane with the first and last being used for field shaping and not connected to the readout.

Figure 2-1 is a schematic of the barrel module showing the key features in the design. Figure 2-3 shows an expanded view of all the components. The measuring planes, each formed of a pair of wafers, are glued to a central TPG baseboard with a thermal conductivity of 1700 W/mK. As shown in the figure, the baseboard protrudes out symmetrically on both sides of the module. The exposed tabs are the points at which the readout hybrids attach to the module. The hybrids form mechanical bridges across the silicon, in a design that reduces the thermal coupling between the front end chips and the silicon without contacting the silicon surface and also avoids gluing to the active surface, given the uncertainties associated with long term ageing and radiation effects.

The cooling contact to the barrel module is made at one side as indicated in the diagrams. The contact point includes dowel pin holes to accurately locate the module on the support structure.



**Figure 2-1** Configuration of the barrel module



**Figure 2-2** Geometry of barrel module detectors and configuration

## 2.2 The forward module

In the forward region, each module is formed from two measuring planes. In the first plane, the azimuthal angle,  $\phi$ , is measured directly via strips of a radial geometry in which the strip pitch varies along the module length. The second measuring plane, identical to the  $\phi$  plane, is mount-

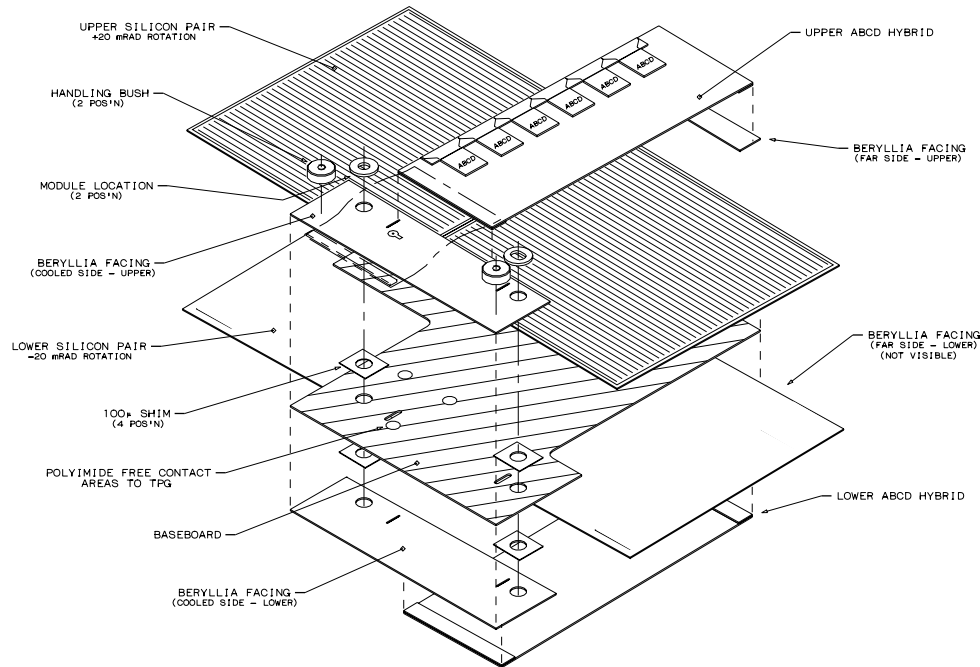


**Figure 2-3** Expanded view of barrel module

ed such that there is a 40 mrad rotation with respect to the  $\phi$  plane. The second plane provides a measure of the radial position of a particle when used in conjunction with the  $\phi$  plane. Figure 2-4 shows a schematic of the wafer dimensions and relative positioning for each of the three module types used in the forward region. Each wheel is covered by one to three rings depending on its  $z$  position in the tracker.

There are 770 strips per measuring plane, with the first and last being used for field shaping and not connected to the readout. Each module subtends an angle larger than that required, to allow for a reasonable number of overlapping strips to ensure hermiticity and to facilitate module-to-module alignment using physics tracks.

Figure 2-5 is a schematic of the forward outer ring module showing the key features in the design. Figure 2-6 is an expanded view of the forward module. The two measuring planes, each formed of a pair of wafers, are sandwiched around a central TPG spine and connected to a double sided hybrid at one end. The TPG spine serves as a mechanical support for the wafers and increases the thermal conductivity along the length of the module. All three designs, the outer, the middle, and the inner modules, are similar except for geometry dependent details. In the case of the outer ring, the electronics is mounted in-board the silicon to maximize the radial coverage allowed within the SCT geometry envelope. The same double sided hybrid is used for all modules. The electrical connections from the silicon strips to the readout electronics are made via fan-in structures mounted on either side of the hybrid bridging the thermal break. The front-end electronics chip-sets are separated into two groups by the primary cooling contact which also serves as the module mounting point. Additional cooling may be provided by a contact to the far end of the spine.

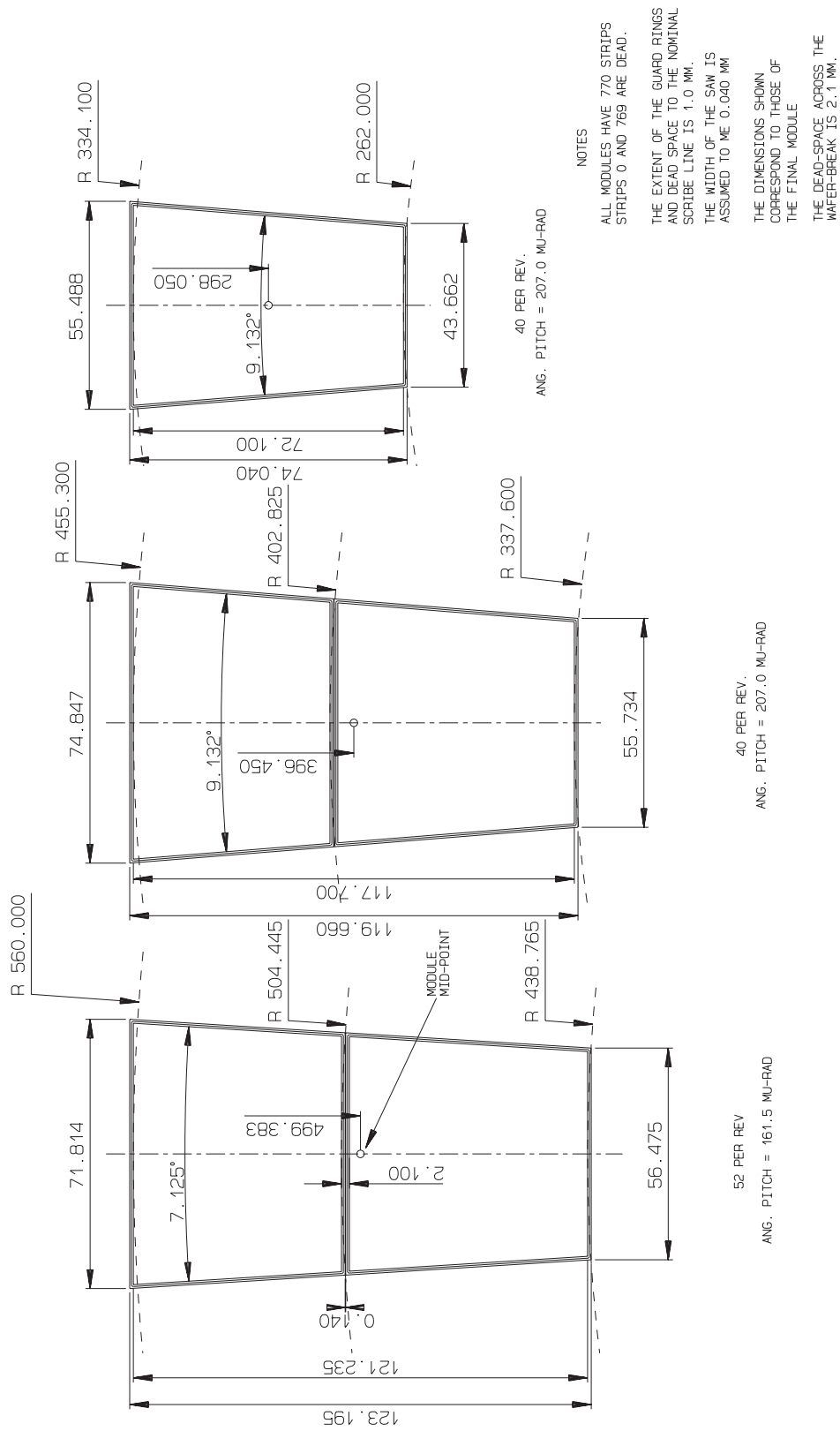
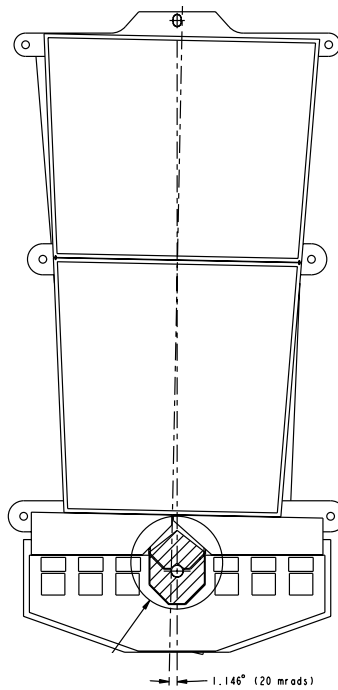
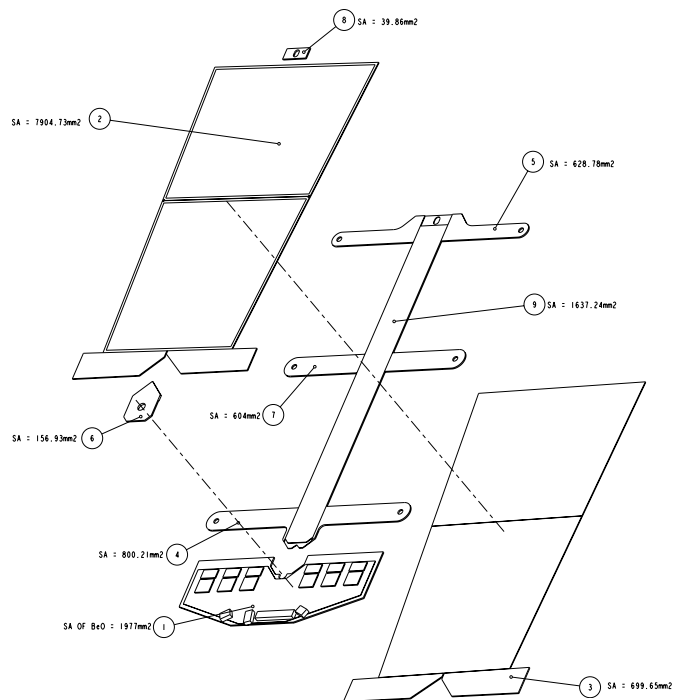


Figure 2-4 Geometry of forward silicon detectors



**Figure 2-5** Forward outer module layout



**Figure 2-6** Expanded view of the forward outer module

### 3. Thermal performance

#### 3.1 Barrel module

A thermal FEA simulation has been carried out for the barrel module design (see Figure 2-1 and Figure 2-3) [1]. Figure 3-1 shows the maximum ( $T_{si\ max}$ ) temperature of the silicon detectors in the module as a function of the bulk heat generation, normalized at  $0^\circ\text{C}$ , for various coolant temperatures. The simulation shows that the thermal runaway of the silicon detector occurs at  $220\ \mu\text{W}/\text{mm}^2$  for the 7.2 W chip power at  $-15^\circ\text{C}$  coolant temperature. Figure 3-2 shows the coolant temperature dependence of the point of thermal runaway. The bulk heat generation after 10 years of operation at LHC is estimated to be  $120\ \mu\text{W}/\text{mm}^2$  in the worst case. The coolant temperature is required to be  $-17^\circ\text{C}$  in order to satisfy the heat generation of  $240\ \mu\text{W}/\text{mm}^2$ , the safety margin of two.

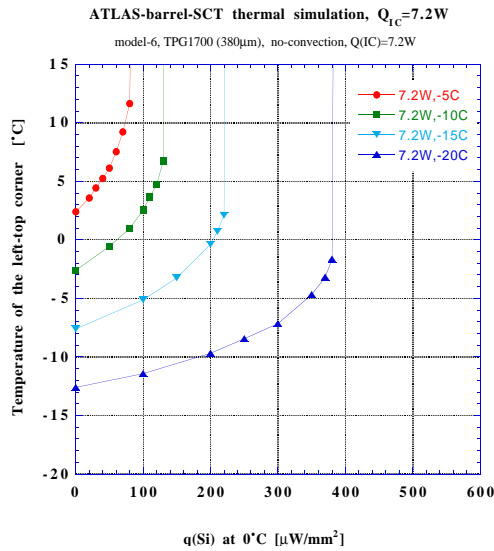


**Figure 3-1** Temperature of the hottest point in the detectors as a function of heat flux, with various coolant temperatures

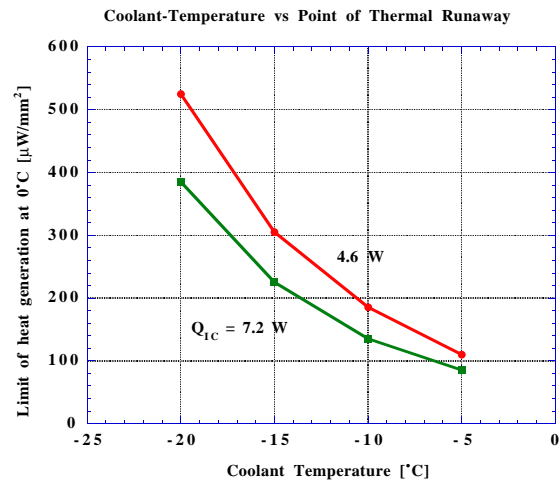


**Figure 3-2** Heat flux at the runaway points as a function of the temperature of coolant

#### 3.2 Forward module

The thermal properties of the outer module (see Figure 2-5 and Figure 2-6) were simulated using FEA analysis [2]. The module is cooled entirely by the cooling blocks. No heat transfer to and from the ambient gas is allowed. The cooling block properties are taken from a separate FEA analysis. The runaway curves for the outer module with 7 W hybrid power is shown in Figure 3-3. The thermal runaway occurs at  $210\ \mu\text{W}/\text{mm}^2$  for the coolant temperature of  $-15^\circ\text{C}$ . A slight decrease of coolant temperature to  $-17^\circ\text{C}$  allows to operate the module at  $240\ \mu\text{W}/\text{mm}^2$ .

### 4. Generic components of modules

Generic components of modules are listed in Table 4-1.



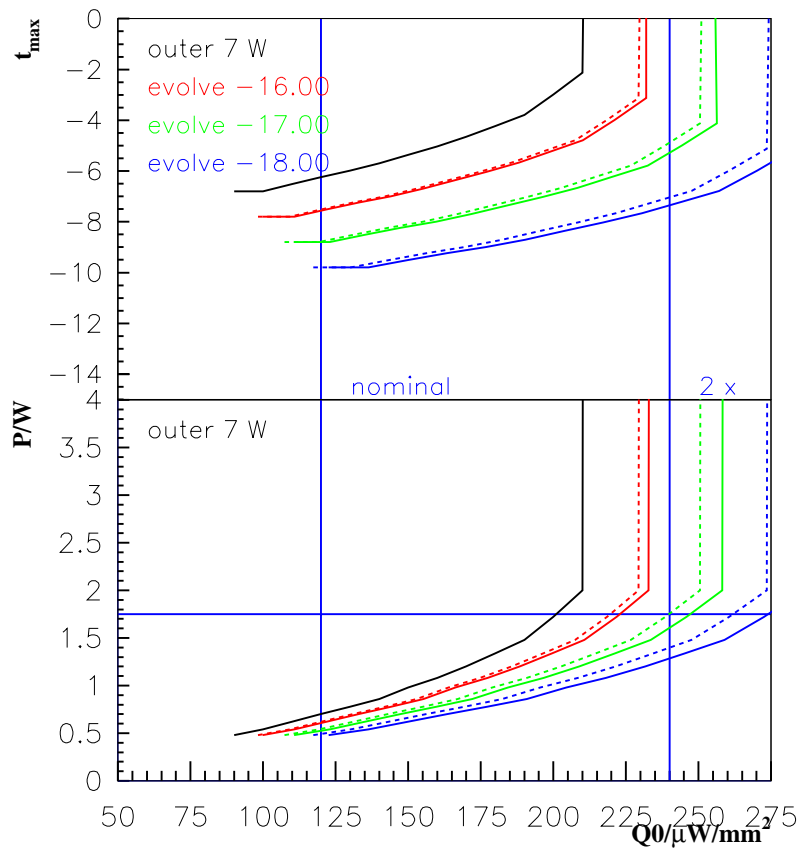


**Figure 3-3** Maximum temperature in the detectors and total power in the outer module for various coolant temperatures for the 7 W hybrid power. The curves are derived from the full simulation at -15 °C using a scaling law. The dashed lines indicate the uncertainties of this scaling.

**Table 4-1** Generic module components

Component	$X_0$ (%)	Contribution (%)
(a) Silicon wafers	0.61	~48
(b) adhesives	0.04-0.06	~4
(c) front end chips	0.04-0.05	~4
(d) thermo-mechanical baseboard	0.18-0.22	~16
(e) hybrid, with bonds and electrical planes	0.30-0.40	~28
Summed material	1.17-1.34	

When considering variations in module components it is vital to ensure that the constructed device is made with high yield, has stable and well-defined geometry, and shows robust electrical performance. The front end electronics and hybrid, coupled with the detailed electrical properties of the wafer will determine the significance of the digitizing precision through the achievable signal-to-noise ratio. The internal mechanical stability and alignment specifications will then limit the ultimate spatial precision that can be achieved for tracks to be used in physics studies. As indicated in Table 4-1 the typical module contribution is 1.26%  $X_0$ . Roughly 20% of the radi-

ation length comes from thermo-mechanical components (b, d) and 80% from electrical elements (a,c,e). Of the latter, 48% are fenced by the need for maximum ionization signal. Any future changes will effect 0.40%  $X_0$  due to refinements in the electrical and mechanical design of the modules with final readout chips etcetera.

## References

- [1] T. Kondo, Thermal FEA simulations for the barrel module
- [2] H-G. Moser, Thermal FEA simulations for the forward modules